

# **EXHIBIT 10**

# GaN-based ultraviolet light-emitting diodes with AlN/GaN/InGaN multiple quantum wells

Hung-Ming Chang,<sup>1</sup> Wei-Chih Lai,<sup>2,3,\*</sup> Wei-Shou Chen,<sup>1</sup> and Shouo-Jinn Chang<sup>1,3</sup>

<sup>1</sup>*Institute of Microelectronics and Department of Electrical Engineering, National Cheng Kung University, Tainan 70101, Taiwan*

<sup>2</sup>*Department of Photonics, National Cheng Kung University, Tainan 70101, Taiwan*

<sup>3</sup>*Advanced Optoelectronic Technology Center, Research Center for Energy Technology and Strategy, National Cheng Kung University, Tainan City 701, Taiwan*  
[weilai@mail.ncku.edu.tw](mailto:weilai@mail.ncku.edu.tw)

**Abstract:** We demonstrate indium gallium nitride/gallium nitride/aluminum nitride (AlN/GaN/InGaN) multi-quantum-well (MQW) ultraviolet (UV) light-emitting diodes (LEDs) to improve light output power. Similar to conventional UV LEDs with AlGaIn/InGaIn MQWs, UV LEDs with AlN/GaN/InGaIn MQWs have forward voltages ( $V_f$ 's) ranging from 3.21 V to 3.29 V at 350 mA. Each emission peak wavelength of AlN/GaN/InGaIn MQW UV LEDs presents 350 mA output power greater than that of the corresponding emission peak wavelength of AlGaIn/InGaIn MQW UV LEDs. The light output power at 350mA of AlN/GaN/InGaIn MQWs UV LEDs with 375 nm emission wavelength can reach around 26.7% light output power enhancement in magnitude compared to the AlGaIn/InGaIn MQWs UV LEDs with same emission wavelength. But 350mA light output power of AlN/GaN/InGaIn MQWs UV LEDs with emission wavelength of 395nm could only have light output power enhancement of 2.43% in magnitude compared with the same emission wavelength AlGaIn/InGaIn MQWs UV LEDs. Moreover, AlN/GaN/InGaIn MQWs present better InGaIn thickness uniformity, well/barrier interface quality and less large size pits than AlGaIn/InGaIn MQWs, causing AlN/GaN/InGaIn MQW UV LEDs to have less reverse leakage currents at  $-20$  V. Furthermore, AlN/GaN/InGaIn MQW UV LEDs have the 2-kV human body mode (HBM) electrostatic discharge (ESD) pass yield of 85%, which is 15% more than the 2-kV HBM ESD pass yield of AlGaIn/InGaIn MQW UV LEDs of 70%.

©2015 Optical Society of America

OCIS codes: (000.0000) General; (000.2700) General science.

## References and links

1. Y. Narukawa, J. Narita, T. Sakamoto, K. Deguchi, T. Yamada, and T. Mukai, "Ultra-high efficiency white light emitting diodes," *Jpn. J. Appl. Phys.* **45**(41), L1084–L1086 (2006).
2. S. D. Lester, F. A. Ponce, M. G. Craford, and D. A. Steigerwald, "High Dislocation Densities in High-Efficiency GaN-Based Light-Emitting-Diodes," *Appl. Phys. Lett.* **66**(10), 1249–1251 (1995).
3. T. Wang, Y. H. Liu, Y. B. Lee, Y. Izumi, J. P. Ao, J. Bai, H. D. Li, and S. Sakai, "Fabrication of high performance of AlGaIn/GaN-based UV light-emitting diodes," *J. Cryst. Growth* **235**(1-4), 177–182 (2002).
4. D. D. Koleske, A. J. Fischer, A. A. Allerman, C. C. Mitchell, K. C. Cross, S. R. Kurtz, J. J. Figiel, K. W. Fullmer, and W. G. Breiland, "Improved brightness of 380 nm GaN light emitting diodes through intentional delay of the nucleation island coalescence," *Appl. Phys. Lett.* **81**(11), 1940–1942 (2002).
5. S. Chichibu, T. Azuhata, T. Sota, and S. Nakamura, "Luminescences from localized states in InGaIn epilayers," *Appl. Phys. Lett.* **70**(21), 2822–2825 (1997).
6. P. R. C. Kent and A. Zunger, "Carrier localization and the origin of luminescence in cubic InGaIn alloys," *Appl. Phys. Lett.* **79**(13), 1977–1979 (2001).
7. M.-K. Kwon, I.-K. Park, S.-H. Beak, J.-Y. Kim, and S. J. Park, "Si delta doping in a GaN barrier layer of InGaIn/GaN multi-quantum-well for an efficient ultraviolet light-emitting diode," *J. Appl. Phys.* **97**(10), 106–109 (2005).

8. A. Knauer, V. Kuehler, S. Einfeldt, V. Hoffmann, T. Kolbe, J.-R. van Look, J. Piprek, M. Weyers, and M. Kneissl, "Influence of the barrier composition on the light output of InGaN multiple-quantum-well ultraviolet light emitting diodes," *Proc. SPIE* **6797**, 67970X (2007).
9. M. Asif Khan, J. W. Yang, G. Simin, R. Gaska, M. S. Shur, and A. Bykhovsky, "Piezoelectric doping in AlInGaN/GaN heterostructures," *Appl. Phys. Lett.* **75**(18), 2806 (1999).
10. M. Kim, M. F. Schubert, Q. Dai, J. K. Kim, E. F. Schubert, J. Piprek, and Y. Park, "Origin of efficiency droop in GaN-based light-emitting diodes," *Appl. Phys. Lett.* **91**(18), 183507 (2007).
11. J. Li, S. L. Shi, Y. J. Wang, S. J. Xu, D. G. Zhao, J. J. Zhu, H. Yang, and F. Lu, "Violet electroluminescence of AlInGaN-InGaN Multiple-quantum-well light-emitting diodes: quantum-confined Stark effect and heating effect," *IEEE Photon. Technol. Lett.* **19**(10), 789–791 (2007).
12. M. Khan, J. W. Yang, G. Simin, R. Gaska, M. S. Shur, H.-C. zur Loye, G. Tamulaitis, A. Zukauskas, D. J. Smith, D. Chandrasekhar, and R. Bicknell-Tassius, "Lattice and energy band engineering in AlInGaN/GaN heterostructures," *Appl. Phys. Lett.* **76**(9), 1161 (2000).
13. Z.-H. Zhang, S. T. Tan, Z. Ju, W. Liu, Y. Ji, Z. Kyaw, Y. Dikme, X. W. Sun, and H. V. Demir, "On the Effect of Step-Doped Quantum Barriers in InGaN/GaN Light Emitting Diodes," *J. Disp. Technol.* **9**(4), 226–233 (2013).
14. R. M. Farrell, P. S. Hsu, D. A. Haeger, K. Fujito, S. P. DenBaars, J. S. Speck, and S. Nakamura, "Low-threshold-current-density AlGaIn-cladding-free *m*-plane InGaN/GaN laser diodes," *Appl. Phys. Lett.* **96**(23), 231113 (2010).
15. Z.-H. Zhang, W. Liu, Z. Ju, S. T. Tan, Y. Ji, Z. Kyaw, X. Zhang, L. Wang, X. W. Sun, and H. V. Demir, "Self-screening of the quantum confined Stark effect by the polarization induced bulk charges in the quantum barriers," *Appl. Phys. Lett.* **104**(24), 243501 (2014).
16. Y. Ji, W. Liu, T. Erdem, R. Chen, S. T. Tan, Z.-H. Zhang, Z. Ju, X. Zhang, H. Sun, X. W. Sun, Y. Zhao, S. P. DenBaars, S. Nakamura, and H. V. Demir, "Comparative study of field-dependent carrier dynamics and emission kinetics of InGaN/GaN light-emitting diodes grown on (11 $\bar{2}$ 2) semipolar versus (0001) polar planes," *Appl. Phys. Lett.* **104**(14), 143506 (2014).
17. L. W. Wu, S. J. Chang, T. C. Wen, Y. K. Su, J. F. Chen, W. C. Lai, C. H. Kuo, C. H. Chen, and J. K. Sheu, "Influence of Si-Doping on the Characteristics of InGaN-GaN Multiple Quantum-Well Blue Light Emitting Diodes," *IEEE J. Quantum Electron.* **38**(5), 446–450 (2002).
18. Z.-H. Zhang, S. T. Tan, Y. Ji, W. Liu, Z. Ju, Z. Kyaw, X. W. Sun, and H. V. Demir, "A PN-type quantum barrier for InGaN/GaN light emitting diodes," *Opt. Express* **21**(13), 15676–15685 (2013).
19. K. Anazawa, S. Hassanet, K. Fujii, Y. Nakano, and M. Sugiyama, "Growth of strain-compensated InGaN/AlN multiple quantum wells on GaN by MOVPE," *J. Cryst. Growth* **370**, 82–86 (2013).
20. H. Z. Ronald A Arif, Y.-K. Ee, and N. Tansu, "Spontaneous Emission and Characteristics of Staggered InGaN Quantum-Well Light-Emitting Diodes," *IEEE J. Quantum Electron.* **44**(6), 573–580 (2008).
21. M. Meneghini, A. Tazzoli, G. Mura, G. Meneghesso, and E. Zanoni, "A Review on the Physical Mechanisms That Limit the Reliability of GaN-Based LEDs," *IEEE Trans. Electron. Dev.* **57**(1), 108–118 (2010).
22. S. Tomiya, T. Hino, S. Goto, M. Takeya, and M. Ikeda, "Dislocation related issues in the degradation of GaN-based laser diodes," *IEEE J. Sel. Top. Quantum Electron.* **10**(6), 1277–1286 (2004).
23. S. N. Lee, H. S. Paek, J. K. Son, H. Kim, K. K. Kim, K. H. Ha, O. H. Nam, and Y. Park, "Effects of Mg dopant on the degradation of InGaN multiple quantum wells in AlInGaN-based light emitting devices," *J. Electroceram.* **23**(2-4), 406–409 (2009).

## 1. Introduction

Gallium nitride (GaN)-based ultraviolet (UV) light-emitting diodes (LEDs) are gaining attention in fields such as UV photolithography, high-density optical data storage, water purification, and portable chemical/biological agent detection/analysis systems. A lattice-mismatched sapphire substrate with a GaN layer induces a high density of the threading dislocations (TDs) during GaN layer growth [1]. Some reports revealed that high TD densities degrade the output power of GaN-based UV LEDs [2,3]. The strong influence of TD on light output was proposed to be caused by reduced localization of minority carriers in quantum wells (QWs) rich in indium (In) and increased trapping at TDs or other nonradiative recombination centers [4]. For blue and green GaN-based LEDs, radiative efficiency is mainly related to the localized states originating from the phase separation or In fluctuation in the InGaN QW [5]. However, the UV LEDs have less localized states than blue and green LEDs because phase separations do not easily occur at low In content. The emission efficiency would be reduced without the assistance of the localized state in InGaN wells low in In of near-UV LEDs. In addition to weak carrier localization effect, the effects of low In content include a much lower potential barrier height of the InGaN/GaN QW in UV LEDs that leads to weak carrier confinement [6,7]. Consequently, the quantum efficiency of a UV LED is drastically decreased with a decrease in In content in the InGaN well. Replacing the InGaN barriers with aluminum (Al) GaN barriers significantly increases the band offset between QWs and barriers resulting in increased efficiency [8]. However, the large lattice

mismatch between AlGa<sub>N</sub> barrier and InGa<sub>N</sub> QW can result in a large piezoelectric and spontaneous polarization field in the QW, thereby reducing the radiative recombination probability of LEDs. Aside from the AlGa<sub>N</sub> barrier of UV LEDs, the AlInGa<sub>N</sub> quaternary barrier has been widely used in short-wavelength UV LEDs because of the characteristics of tuning band, strain, and internal field in the wells [9–18]. Increase in the band offset for the UV LED MQWs enhances carrier confinement and then improves emission efficiency. AlN barrier can generate large band offset for the application of the UV LED MQWs. However, material combination with a big difference in lattice constants, like InGa<sub>N</sub>/AlN MQWs, has rarely been chosen for well and barrier layers. It would have large strain and thus strong piezoelectric field in each of the InGa<sub>N</sub> and AlN layers; moreover, growth conditions (e.g., temperature) of both materials are quite different, making it difficult to obtain good quality of heterostructure. Anazawa et al. have reported the strain-compensated AlN/InGa<sub>N</sub> MQWs [19]. InGa<sub>N</sub> layer would compress the Ga<sub>N</sub> and AlN layers and tense Ga<sub>N</sub>. Therefore, AlN/InGa<sub>N</sub> would have a strain-compensated multiheterostructure to Ga<sub>N</sub>. However, the thickness of the each layer should be precisely controlled to have strain-compensated AlN/InGa<sub>N</sub> MQWs. The piezoelectric field would appear once we miss the prescribed thickness for each layer of the strain-compensated AlN/InGa<sub>N</sub> MQWs. Arif et al. have reported the staggered QW structure to deal with the internal field of the wells [20]. The staggered QW structure could improve the electron hole overlap in the QWs with internal field. Therefore, we would like to introduce UV LEDs with AlN/GaN/InGa<sub>N</sub> MQW structure to replace AlGa<sub>N</sub>/InGa<sub>N</sub> MQW of UV LEDs. The effects of the UV LEDs with AlN/GaN/InGa<sub>N</sub> MQW structure on the electrical and optical properties of the Ga<sub>N</sub>-based UV LEDs, as well as the fabrication process are discussed in this paper.

## 2. Experiment

All samples were grown on a 2-in (0001) patterned sapphire substrate (PSS) through a Thomas Swan close-coupled showerhead  $31 \times 2$  metalorganic chemical vapor deposition (MOCVD) system. The PSS periodic convex pattern was formed using an inductively coupled plasma etcher. Pattern diameter, spacing, and height of the PSS were 2.5, 1, and 1.6  $\mu\text{m}$ , respectively. During MOCVD growth, trimethylindium, trimethylgallium, trimethylaluminum, and ammonia were used as the source materials of In, Ga, Al, and N, respectively. Bicyclopentadienyl magnesium and silane were used as the p-type and n-type doping sources. The reactor temperature was raised to 500  $^{\circ}\text{C}$  to grow a 20 nm-thick Ga<sub>N</sub> nucleation layer on the PSS in situ. The reactor temperature was then raised to 1050  $^{\circ}\text{C}$  to grow a 2  $\mu\text{m}$ -thick undoped Ga<sub>N</sub> epitaxial layer followed by the deposition of a 2  $\mu\text{m}$ -thick n-GaN layer. Subsequently, a nine-pair InGa<sub>N</sub> (2.5 nm)/AlGa<sub>N</sub> (4.5 nm) UV light-emitting MQW structures, named conventional UV LEDs, was produced via a high–low temperature scheme. The growth temperatures of AlGa<sub>N</sub> and AlN/GaN barrier layers were kept at 820  $^{\circ}\text{C}$ . The growth pressures for AlGa<sub>N</sub>/InGa<sub>N</sub> and AlN/GaN/InGa<sub>N</sub> MQWs are 300 mbar. We varied the growth temperature of the InGa<sub>N</sub> well from 800  $^{\circ}\text{C}$  to 770  $^{\circ}\text{C}$  to have the UV LEDs emission wavelength of 375, 385, and 395 nm. After the growth of the light-emitting MQWs structure, an AlGa<sub>N</sub> electron blocking layer (EBL) was grown on AlGa<sub>N</sub>/InGa<sub>N</sub> MQWs and AlN/GaN/InGa<sub>N</sub> MQWs. The details UV LEDs structure, growth temperatures of MQWs, and source-switching sequences of the AlGa<sub>N</sub>/InGa<sub>N</sub> and AlN/GaN/InGa<sub>N</sub> MQWs are showing in the Fig. 1(a) and 1(b), respectively. Thickness and Al% of the AlGa<sub>N</sub> barrier were approximately 4.5nm and 15%, respectively. The expected thicknesses of the AlN and Ga<sub>N</sub> for the AlN/GaN barrier are approximately 2.5nm and 2.0nm, respectively. A 0.1 $\mu\text{m}$ -thick p-GaN layer was deposited following the EBL layer.

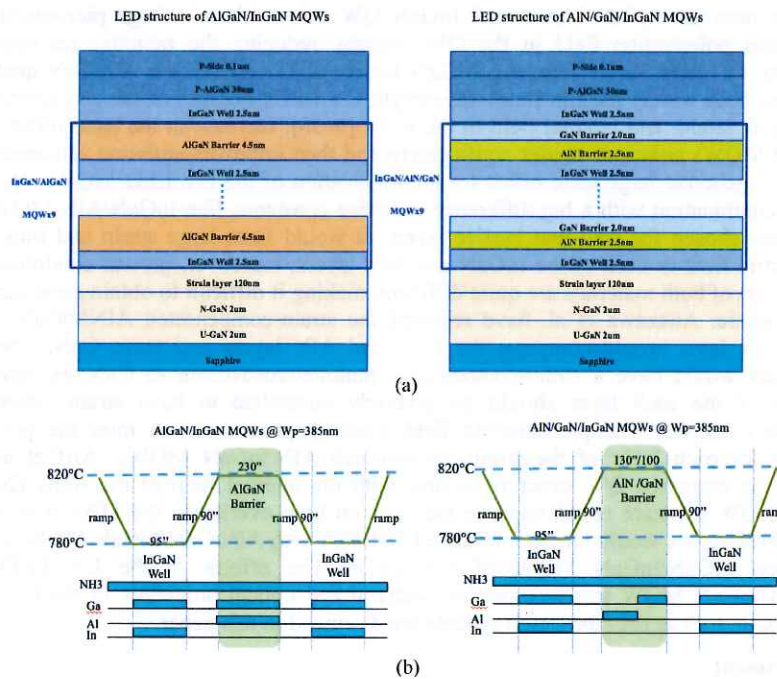


Fig. 1. (a) UV LEDs structure of the AlGaIn/InGaIn and AlN/GaN/InGaIn MQWs. (b) The growth temperatures and source-switching sequences of the AlGaIn/InGaIn and AlN/GaN/InGaIn MQWs.

Subsequently, standard processing steps were performed to fabricate  $1143 \mu\text{m} \times 1143 \mu\text{m}$  LED chips with indium tin oxide in the upper contact. The current–voltage (I–V) characteristics of the fabricated LEDs were then measured using an HP-4156C semiconductor parameter analyzer with a 100-mA current limit. At a high current injection, a Keithley 2400 source meter was used to measure the I–V characteristics of these LEDs. The output power and emission wavelength of the LEDs were measured at room temperature using a calibrated integrating sphere and a spectrometer (Ocean Optics USB2000).

### 3. Results and discussion

Figure 2(a) reveals the I–V characteristics of GaN-based UV LEDs with AlGaIn/InGaIn and AlN/GaN/InGaIn MQWs. All UV LEDs with AlGaIn/InGaIn and AlN/GaN/InGaIn MQWs showed forward voltages ( $V_f$ ) in the range of 3.21 V to 3.29 V at 350 mA. The ideality factors of the forward I–V characteristics of UV LEDs with AlGaIn/InGaIn MQWs in the applied voltage range of 3.23 V to 3.31 V ranged between 1.75 and 1.78. However, UV LEDs with AlN/GaN/InGaIn MQWs revealed a smaller ideality factor in the range of 1.62 and 1.73 compared with that of UV LEDs with AlGaIn/InGaIn MQWs. The improved ideality factor of the UV LED with AlN/GaN/InGaIn MQWs indicates less defect-related leakage current recombination. Moreover, Fig. 2(b) shows that the reverse leakage currents at –20 V of UV LEDs with AlGaIn/InGaIn and AlN/GaN/InGaIn MQWs ranged between –1900 to –5000 nA and –98 to –385 nA, respectively. The reverse leakage current at –20 V of the UV LED with AlN/GaN/InGaIn MQWs was nearly two orders less than that of the UV LED with AlGaIn/InGaIn MQWs.

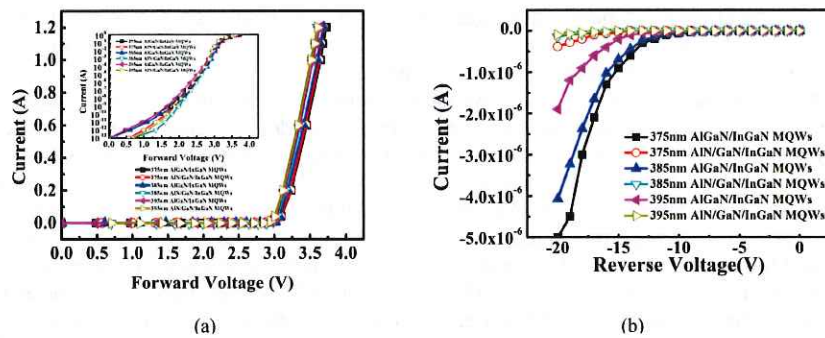


Fig. 2. (a) Forward I-V and (b) reverse I-V characteristics of GaN-based UV LEDs with AlGaIn/InGaIn and AlN/GaN/InGaIn MQWs.

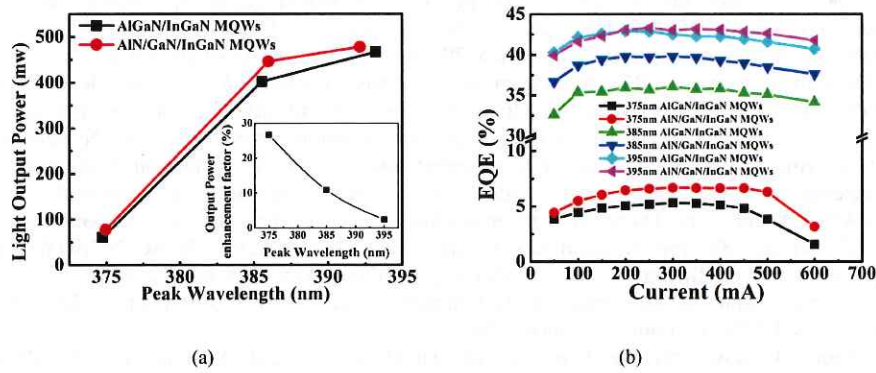


Fig. 3. (a) Output power of UV LEDs at 350-mA current injections and (b) external quantum efficiency (EQE) of UV LEDs with AlGaIn/InGaIn and AlN/GaN/InGaIn MQWs. The inset in Fig. 3 (a) shows the emission wavelength dependent the output power enhancement factor.

Figure 3(a) shows the light output powers of UV LEDs at 350-mA current injections as a function of emission peak wavelength. The light output powers of 374.74, 385.55, and 393.2 nm of AlGaIn/InGaIn MQW of UV LEDs were 60.81, 402.32, and 466.65 mW, respectively. In addition, the light output powers at the emission peak wavelength 374.94, 385.98, 392.13 nm of UV LEDs with AlN/GaN/InGaIn MQWs were 77.05, 445.96, 478.0 mW, respectively. It is found that the AlN/GaN/InGaIn MQWs UV LEDs have larger 350-mA light output power than that of AlGaIn/InGaIn MQW UV LEDs for the all emission peak wavelength. One of reasons for the improved 350-mA light output power of AlN/GaN/InGaIn MQWs UV LEDs can be attributed to the staggered QW structure of AlN/GaN/InGaIn MQWs. The staggered QW structure could improve the electron hole overlap in the QWs with internal field [20]. The UV LEDs with AlGaIn/InGaIn and AlN/GaN/InGaIn MQWs degraded their 350-mA light output power as the emission peak wavelength shortened, which could be attributed to the increased influence of the dislocation of the n-GaN layers and the weak carrier confinement of the QW. We take a look at the emission peak wavelength dependent average output power enhancement factor showing in inset of Fig. 3(a), which is defined the light output power differences between AlN/GaN/InGaIn MQWs UV LEDs and AlGaIn/InGaIn MQWs UV LEDs at 350 mA divided by the light output power of AlGaIn/InGaIn MQWs UV LEDs at 350 mA. It is found that the enhancement factor of the 350-mA output power of AlN/GaN/InGaIn MQW UV LEDs increased as the emission peak wavelength decreased as shown in the inset in Fig. 3(a). The output power enhancement factor can reach around 26.7% at the emission peak wavelength of 375 nm but reach only

around 2.43% at emission peak wavelength of 395 nm. The results show that the light output power of the LEDs with short-peaked UV wavelength is improved by AlN/GaN/InGaN MQWs because of the enhanced carrier confinement.

AlN/GaN/InGaN MQW UV LEDs would also improve light output power at high current injection. Figure 3(b) shows the injection current-dependent external quantum efficiency (EQE) of the 375-, 385-, and 395-nm emission wavelength UV LEDs with AlGaIn/InGaIn and AlN/GaN/InGaIn MQWs. AlN/GaN/InGaIn MQW UV LEDs with 395-nm emission wavelength shows less EQE than AlGaIn/InGaIn MQW UV LEDs at an injection current below 200 mA. When the injection current is larger than 200 mA, the EQE of AlN/GaN/InGaIn MQW UV LEDs with 395-nm emission wavelength becomes larger than that of AlGaIn/InGaIn MQW UV LEDs. The AlN/GaN barrier may cause more lattice mismatch in InGaIn wells with 395-nm emission wavelength, resulting in the crystal quality degradation of InGaIn wells or increase the piezoelectric field in InGaIn wells. It would also degrade the EQE of UV LEDs under low current injection. However, for InGaIn wells with 395-nm emission wavelength, AlN/GaN barrier would have better carrier confinement than the AlGaIn barrier under high current injection. It would cause the 395-nm emission wavelength UV LEDs with AlN/GaN/InGaIn MQWs to have larger EQEs than AlGaIn/GaN MQWs at an injection current more than 200 mA. However, AlN/GaN/InGaIn MQW UV LEDs with 375-nm and 385-nm emission wavelengths have larger EQEs than AlGaIn/InGaIn MQW UV LEDs with emission wavelengths of 375 nm and 385 nm at all injection current levels. The carrier confinement of the AlGaIn barrier would be good for InGaIn wells with 395-nm emission wavelength under low current injection. With a reduction in the emission wavelength of UV LEDs, the strain within InGaIn wells would be reduced for both AlGaIn and AlN/GaN barriers. Therefore, carrier confinement would become the dominant effect of the 375-nm and 385-nm emission wavelength UV LEDs. As AlN/GaN/InGaIn MQWs have superior carrier confinement than AlGaIn/InGaIn MQWs, AlN/GaN/InGaIn MQW UV LEDs with 375-nm and 385-nm emission wavelengths have larger EQEs than AlGaIn/InGaIn MQWs UV LEDs at all injection current levels.

Figure 4 shows the SEM images of AlGaIn/InGaIn and AlN/GaN/InGaIn MQWs. AlGaIn/InGaIn MQWs have large pits each with a size of around 1.3  $\mu\text{m}$  based on low magnification SEM observation. By contrast, AlN/GaN/InGaIn MQWs do not show any large-sized pits on the surface under the same SEM observation condition. However, AlN/GaN/InGaIn and AlGaIn/InGaIn MQWs exhibit small pits each with a size of around 90

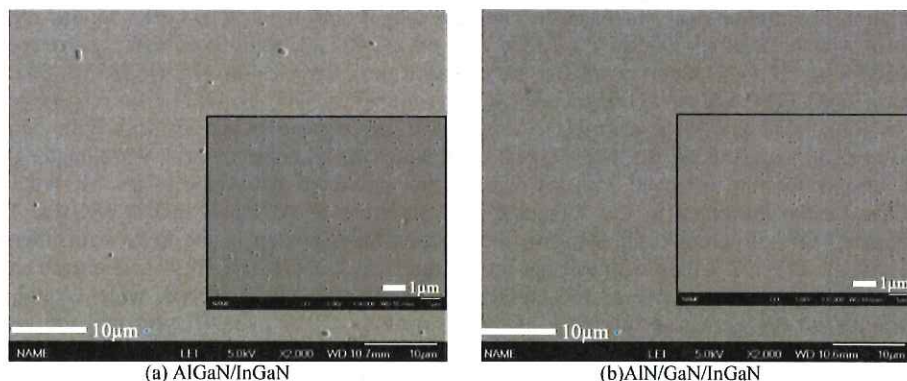


Fig. 4. SEM images of the surfaces of (a) AlGaIn/InGaIn and (b) AlN/GaN/InGaIn MQWs. The insets in (a) and (b) are enlarged SEM images of the smooth surface areas of AlGaIn/InGaIn and AlN/GaN/InGaIn MQWs, respectively.

nm on the surface when we zoomed in on the smooth area of both samples as shown in the insets in Figs. 4(a) and 4(b), respectively. Furthermore, AlN/GaN/InGaIn MQWs have a pit

density of  $1.01 \mu\text{m}^{-2}$ , which is smaller than AlGaIn/InGaIn MQWs' pit density of  $2.01 \mu\text{m}^{-2}$ . To understand the microstructure of AlGaIn/InGaIn and AlIn/GaN/InGaIn MQWs we have fulfilled the high resolution transmission electron microscope (HRTEM) (FEI Tecnai F20 TEM) observation on AlGaIn/InGaIn and AlIn/GaN/InGaIn MQWs UV LEDs with emission peak wavelength of 385nm. Figure 5 (a) and 5(b) show the TEM images of the AlGaIn/InGaIn and AlIn/GaN/InGaIn MQWs UV LEDs, respectively. The thicknesses of the InGaIn wells measured from HRTEM images ranging from 2.5 to 3.0 nm meet the designed deposition conditions. It is found that the AlGaIn/InGaIn MQWs does not show a steep interface between the AlGaIn and InGaIn layer. And the InGaIn wells thickness shows a significant fluctuation in the AlGaIn/InGaIn MQWs. In contrast, the AlIn/GaN/InGaIn MQWs shows a clear interface between the AlIn/GaN barrier and InGaIn wells. And the InGaIn wells thickness indicates a better uniformity in the AlIn/GaN/InGaIn MQWs. Therefore, the enhanced 350mA light output power of the AlIn/GaN/InGaIn MQWs UV LEDs is considered to result from the better barrier/well interfacial structure and thickness uniformity of AlIn/GaN/InGaIn MQWs than those of AlGaIn/InGaIn MQWs. However, we could not reveal the individual AlIn layer and GaN layer in our designed AlIn/GaN barrier from the HRTEM images. One of reasons for this problem is attributed to the composition fluctuation in each atomic layer deposited by MOCVD. So, composition fluctuation exists in layers of MQW, and results in no defined boundaries between AlIn-GaN in HRTEM images. The other reason for this problem might be from that the Al atoms and Ga atoms might inter-remix or inter-diffuse with the in front GaN layer during the AlIn growth. Energy dispersive X-ray (EDX) line profiles by scanning transmission electron microscope (STEM) mode from both UV LEDs samples, as shown in Fig. 6, displayed the elemental distribution of the Al, In, and Ga atoms through a distance of 50 nm in both AlGaIn/InGaIn MQWs and AlIn/GaN/InGaIn MQWs. These results indicated that the composition iteration in AlIn/GaN/InGaIn MQWs is more controllable in processes of deposition and annealing due to those Al rich layers. It could also improve the carrier confinement of the UV LEDs by introducing AlIn/GaN/InGaIn MQWs.

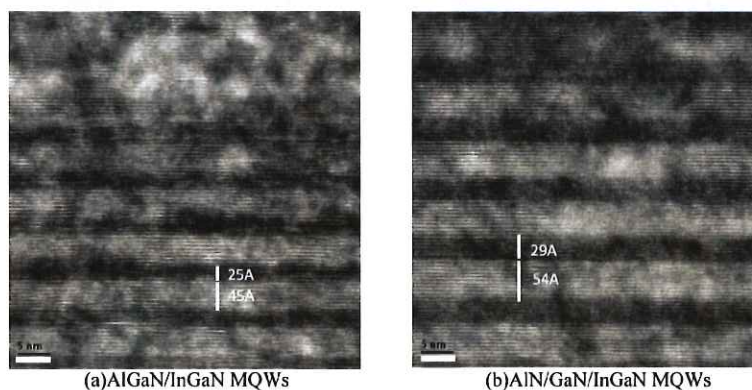


Fig. 5. The TEM images of the (a) AlGaIn/InGaIn MQWs and (b) AlIn/GaN/InGaIn MQWs.

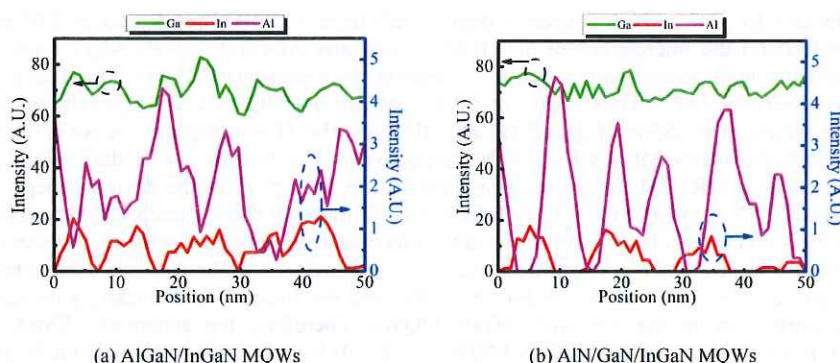


Fig. 6. EDX line profiles by STEM mode from the (a) AlGaIn/InGaIn MQWs and (b) AlN/GaN/InGaIn MQWs UV LEDs samples.

AlN/GaN/InGaIn MQWs have better InGaIn thickness uniformity, well/barrier interface quality and less large size V-shaped pit density (size more than  $1\ \mu\text{m}$ ) than AlGaIn/InGaIn MQWs. These effects might be the reasons behind AlN/GaN/InGaIn MQW UV LEDs having less reverse leakage currents at  $-20\text{V}$ . Also worth noting is that AlN/GaN/InGaIn MQW UV LEDs have the 2-kV human body mode (HBM) electrostatic discharge (ESD) pass yield of 85% which is 15% more than the 2-kV HBM ESD pass yield of AlGaIn/InGaIn MQW UV LEDs of 70%. The improved ESD pass yield should be again attributed to better interface quality and less large size V-shaped pit density than AlGaIn/InGaIn MQWs.

Figure 7 indicates the light output and reverse leakage of current reliabilities of the emission peak wavelength 385 nm of UV LEDs with AlN/GaN/InGaIn MQWs and AlGaIn/InGaIn MQWs. The UV LEDs were aged at 350 mA of injection current at  $80^\circ\text{C}$  for 196 h. Within 196 h, AlN/GaN/InGaIn MQW UV LEDs revealed an output power drop of around 3.6%, which is less than the approximated 8.7% output power drop of AlGaIn/InGaIn MQW UV LEDs [Fig. 7(b)]. The reverse leakage currents at  $-5\text{ V}$  of the AlN/GaN/InGaIn MQW and AlGaIn/InGaIn MQW UV LEDs [Fig. 7(a)] increased with the aging time. However, the AlGaIn/InGaIn MQW UV LEDs demonstrated much larger reverse leakage current increments with the aging time than AlN/GaN/InGaIn MQW UV LEDs. Meneghini et

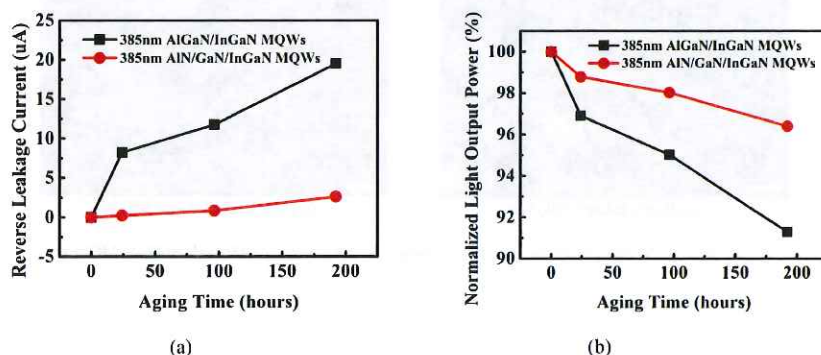


Fig. 7. (a) Reverse leakage current at  $-5\text{V}$  and (b) light output power reliability of UV LEDs with AlGaIn/InGaIn and AlN/GaN/InGaIn MQWs.

al [21], have reported that generation defects and doping redistribution in the active region would degrade the power output and increase the reverse leakage current of UV LEDs during electrical aging. Reports presented evidence for the diffusion of doping/impurities (e.g., Mg and Si) toward the active region of LEDs [22,23] and suggested that the presence of defects

play a significant role in easing the diffusion process even at relatively low temperatures [21]. AlN/GaN/InGa<sub>N</sub> MQWs have better InGa<sub>N</sub> thickness uniformity, well/barrier interface quality and less large size V-shaped pit density than AlGa<sub>N</sub>/InGa<sub>N</sub> MQWs. Therefore, the improved reliability of AlN/GaN/InGa<sub>N</sub> MQW UV LEDs can again be attributed to better InGa<sub>N</sub> thickness uniformity, well/barrier interface quality and less large size V-shaped pit density of AlN/GaN/InGa<sub>N</sub> MQWs.

#### 4. Conclusion

In summary, we have demonstrated that AlN/GaN/InGa<sub>N</sub> MQW UV LEDs can improve light output power. UV LEDs with AlN/GaN/InGa<sub>N</sub> MQWs have 350-mA forward voltages ( $V_f$ ) in the range of 3.21 V to 3.29 V, which are similar to those of conventional AlGa<sub>N</sub>/InGa<sub>N</sub> MQW UV LEDs. The 350-mA output power at each emission peak wavelength of AlN/GaN/InGa<sub>N</sub> MQW UV LEDs is greater than that of the corresponding emission peak wavelength of AlGa<sub>N</sub>/InGa<sub>N</sub> MQW UV LEDs. The light output power enhancement can reach around 26.7% in magnitude at the emission peak wavelength of 375 nm, but can reach only around 2.43% at emission peak wavelength of 395 nm. Moreover, compared with AlGa<sub>N</sub>/InGa<sub>N</sub> MQWs, AlN/GaN/InGa<sub>N</sub> MQWs present better InGa<sub>N</sub> thickness uniformity, well/barrier interface quality and less large size pits, thereby having less reverse leakage currents at -20V. AlN/GaN/InGa<sub>N</sub> MQW UV LEDs also have 2-kV HBM ESD pass yield of 85%, which is larger than AlGa<sub>N</sub>/InGa<sub>N</sub> MQW UV LEDs' 70% 2-kV HBM ESD pass yield. In addition, AlN/GaN/InGa<sub>N</sub> MQW UV LEDs demonstrate improved reliability characteristic. AlN/GaN/InGa<sub>N</sub> MQW UV LEDs show a light output power drop of around 3.6%, whereas AlGa<sub>N</sub>/InGa<sub>N</sub> MQW UV LEDs exhibit 8.7% light output power drop within 196 h.

#### Acknowledgments

The authors are grateful to the National Science Council of Taiwan for their financial support under Contract Nos. NSC101-2221-E-006-066-MY3 and 102-3113-P-009-007-CC2. This research was also made possible through the Advanced Optoelectronic Technology Center, National Cheng Kung University, as a project of the Ministry of Education of Taiwan, and through the financial support of the Bureau of Energy, Ministry of Economic Affairs of Taiwan, under Contract No. 102-E0603. We would like to especially thank Dr. J. S. Bow for performing the TEM observation on AlGa<sub>N</sub>/InGa<sub>N</sub> and AlN/GaN/InGa<sub>N</sub> MQWs UV LEDs.